Building blocks of self-organized criticality, part I: the very low drive case

Ryan Woodard* and David E. Newman
University of Alaska Fairbanks
Fairbanks, Alaska 99775-5920, USA

Raúl Sánchez
Universidad Carlos III de Madrid
28911 Leganés, Madrid, Spain

Benjamin A. Carreras
Oak Ridge National Laboratory
Oak Ridge, Tennessee 37831-8070, USA
(Dated: July 9, 2004)

We describe new analyses and signatures of the self-organized critical one dimensional directed running sandpile model of Hwa and Kardar [Phys. Rev. A **45**, 7002 (1992)]. We present results for extremely low levels of external forcing of this SOC model and show that correlations in the dynamics exist over very long time scales regardless of how low this driving rate is. This demonstrates that a SOC system has nontrivial dynamics even when the system's events do not overlap in space or time. A consequence of this is that the power spectral and rescaled range (R/S) analysis signatures of the SOC time series for very weak forcing are very different from a simple random superposition of pulses.

PACS numbers: 05.65.+b, 05.40.-a, 52.25.Fi, 96.60.Rd

I. INTRODUCTION

Self-organized criticality (SOC) [1, 2] is a dynamical framework that describes how certain large-scale complex behaviour can emerge from a system of small-scale simple interactions. SOC concerns the dynamics of nonequilibrium systems that have a local critical threshold. If this threshold is constant throughout the entire system, then an average constant global gradient is maintained through two opposing mechanisms: an external forcing that increases the gradient and internal transport of the quantity that reduces the gradient. The relaxation of the gradient usually occurs in a series of aperiodic bursts, called avalanches in SOC lingo. The avalanche mechanism allows for stable gradients to exist in the system and contrasts with linear diffusion, which constantly acts to reduce any gradient. In SOC, the avalanches take place on time scales that are much shorter than those of the external forcing.

Books [3, 4] and numerous papers [5, 6] have been written to give detailed overviews of SOC. To get a flavor of the potential generality of the theory, an oft-used shortcut is to look at examples of the different systems that have been studied as possibly SOC. Such systems include, among others, confined fusion plasmas [7–10], the magnetosphere [11–13], tectonic systems [14], electrical power networks [15–17] and communication networks [18]. Note how very different these systems are from each other and that entire fields of study are devoted to separately understanding them. In short, what all of these systems seem to have in common are gradients that build up and persist and are then reduced in relatively quick bursts of activity. The signatures of some measures of this avalanching activity are remarkably similar in systems proposed as SOC.

SOC may be, then, a common mechanism in many different physical systems. To investigate whether or not a system is consistent with SOC, a defined model must be used to compare its signatures and features with those of the system under study; there are many SOC models. The rest of this paper is devoted to analyzing one such model, the one dimensional directed running sandpile.

[19] studied this model for strong external forcing and found that when avalanche events overlap in space and time there is a hydrodynamic regime of intermediate time scales over which long time correlations in the dynamics exist. These time scales are greater than the longest duration of a single avalanche and the power spectrum in this region is shown to scale as $1/f$. This is important because power law scaling of the spectrum is one of the common features of systems proposed to be SOC and the specific $1/f$ scaling of many systems has been a longstanding puzzle since before the introduction of SOC (see, for instance, [20]). [19] also looked at weak forcing, when single events do not overlap in space or time, and found that the signatures of their sandpile model at weak forcing are consistent with those of random superpositions of pulses (an analytical treatment of this is given

*Electronic address: ryan@timehaven.org

in [21] and [22]). That study concludes that overlapping is necessary in order for this system to have "interesting temporal fluctuations such as $1/f$ noise. . . ."

In contrast, we will show that interesting, nontrivial dynamics can exist at all driving rates in this system, including extremely weak forcing when single events do not overlap in time. To do so we have to probe very long time scales where the dynamics and effects of weak forcing appear. We find that the strong forcing case studied previously is the limiting case of the more fundamental weak forcing results presented here. Specifically, we will show that a SOC time series cannot simply be approximated by a random superposition of pulses or signals. Long time correlations among separate avalanches always exist in the series regardless of the strength of the external forcing and regardless of whether or not avalanches overlap in time. The correlations are due to memory stored in the local gradients of the system. We quantify correlations with the power spectrum and rescaled range analysis and find that the latter is a more consistent measure of correlated dynamics than the former. The comparison of these two measures reveals that the dynamics that produces a $1/f$ region at high drive is also present at low drive, though now the spectrum scales as $f^{-\beta}$ with $\beta < 1$.

II. MODEL

The prototypical SOC model is known as the sandpile. The name was chosen to produce a good, simple mental picture, not because it necessarily models real sandpiles. There are many varieties of sandpile models [2, 4, 23]; we will only describe the one dimensional directed running sandpile of [19]. In addition to general SOC theory, this model is useful in studying physical systems where the dynamics can be reduced to a one dimensional approximation. One example of this is a fusion plasma confined in a tokamak [7, 24], where, because of toroidal and poloidal symmetries, plasma transport can be approximated by a steady gradient in one dimension. The single dimension can represent gradient-driven turbulent transport of plasma, heat and density from the hot dense core to the cooler, less dense edge of the tokamak.

Consider a single column of L cells. Each cell contains an integer number of "sand grains"; this number is the height of the cell. Sand is added to each cell by a "rain" U_0 from above. That is, at each time step for each cell, there is a probability $0 < P_0 < 1$ that U_0 grains of sand will be added to it. The units of P_0 are grains per time step per cell. Average input current into the entire system is then $\overline{J_{\rm IN}} = P_0 L$ grains per time step. The local gradient $Z_{\rm n}$ is the difference in height between two neighboring cells. If this local gradient exceeds a critical gradient $Z_{\rm crit}$ then an avalanche occurs. An avalanche stabilizes the local gradient by transferring $N_{\rm f}$ grains of sand from the higher cell to the lower. This avalanche can make $Z_{\rm n+1}$ and/or $Z_{\rm n-1}$ unstable at the next time step so that the avalanche spreads to other cells. In this way, spatially and temporally extended events in a system can occur. This sandpile can be extended to two or more dimensions [2] but, again, we will only discuss the one dimensional case.

The time scales of the external drive and the internal relaxations are well-separated in a defined SOC system. For the sandpile, this can be accomplished in two ways: by using the zero drive model or by using the running sandpile model with low driving rate. In the zero drive model, the rain of sand is suspended ($P_0 \to 0$) when an avalanche is taking place. This ensures the separation of time scales needed in a SOC process but clouds the meaning of one time step. In contrast, time is well-defined in the running sandpile, where the rain of sand continues with the same probability even when an avalanche is taking place. For this study, the fixed parameters are $U_0 = 1$, $Z_{\rm crit} = 8$ and $N_{\rm f} = 3$. We explore a parameter space of the two remaining parameters, system size L and probability P_0.

The time series that we analyze is called the flips—all of the analyses in this paper are of this specific type of sandpile data. Flips are defined as the total number of unstable sites (where $Z \geq Z_{\rm crit}$) at each time step in a sandpile model in steady state. An unstable cell flips $N_{\rm f}$ grains of sand to the next cell. The total flips at each time step can be thought of as the instantaneous (potential) energy dissipation in the system. Avalanches in a flips time series appear as structures—multiple sequential nonzero flips separated by periods of inactivity, or quiet times. Quiet times are Poisson distributed because of the random drive of the system. See [25, 26] for detailed discussions of quiet times.

III. METHODS

This model is a dynamical system; a characteristic of such systems that can quantify the dynamics is long time correlations. We study long time correlations with the power spectrum and rescaled range (R/S) analysis. The power spectrum is defined as the square of the Fourier transform, $S(f) = |F(f)|^2$, where $F(f) = N^{-1}\sum_{t=0}^{N-1} X(t)e^{-i2\pi(f/N)t}$. For a finite real time series, the spectrum also equals the Fourier transform of the autocorrelation function of the time series.

What does the power spectrum say about correlations in a series? More appropriate here, what does a power spectrum that scales as a power law $f^{-\beta}$ have to say about correlations in a series? We can qualitatively answer this. For $\beta > 0$, the low frequencies are more important in the dynamics so the series tends to look relatively smooth and trends persist. Such series are said to be correlated. For $\beta < 0$, the high frequency components are more important and the series is very rough. Trends do not persist long and the series is called anticorrelated. Truly random noise, with neither correlations nor anticorrelations, has a spectrum that scales with $\beta = 0$.

Another measure of correlations is the Hurst exponent, $H \in (0,1)$ [27]. A value of $H > 0.5$ implies correlated dynamics, $H < 0.5$ anticorrelated and $H = 0.5$ uncorrelated. Opinions in the literature differ over which method is best for calculating H. Each of the various methods has strengths and weaknesses. We measure H by using R/S analysis [27–29], though there are other techniques, such as scaled window variance [30], detrended fluctuation analysis [31] and structure functions [32]. For reference, an application of using R/S analysis to calculate H is in evaluating various computer algorithms for pseudorandom number generators (PRNGs) [33]. In that study, the quality of various PRNGs is evaluated based on the length of a data series that can be produced where $H \approx 0.5$.

The rescaled range is defined as $R'(\tau) \equiv R(\tau)/S(\tau)$, where $S(\tau)$ is the standard deviation and

$$R(\tau) = \max_{1\le k\le\tau} W(k,\tau) - \min_{1\le k\le\tau} W(k,\tau) \quad \text{(range)},$$

$$W(k,\tau) = \sum_{t=1}^{k} (X_t - \langle X\rangle_\tau) \ \text{(cumulative deviation) and}$$

$$\langle X\rangle_\tau = \frac{1}{\tau}\sum_{t=1}^{\tau} X_t \quad \text{(mean)}.$$

If the rescaled range of the time series scales as $R'(\tau) \sim \tau^H$, the slope of the plot of $R'(\tau)$ versus the time lag τ on a doubly logarithmic plot is the Hurst exponent, H. We use both the power spectrum and R/S analysis to characterize correlations.

IV. RESULTS

The study reported here is of the SOC sandpile model for very low external forcing. Very low drive can be defined empirically by examining the flips time series and choosing cases where individual avalanches are distinct and well-separated by quiet times, that is, where there is no overlapping of events.

In [34], we show that this criterion is satisfied by $P_0L^2 \ll 1$, where P_0L^2 is the *effective driving rate*. We use P_0L^2 instead of the average input rate P_0L because the former takes into account both the total flux into the system and the system size itself. This is important because a given total flux P_0L that, for a large system, is weak enough that avalanches do not overlap in time may actually be very strong for a much smaller system so that avalanches do overlap in time. Therefore, P_0L is effectively larger for a smaller system. Using the effective driving rate allows systems of different sizes and strengths of forcing to be compared.

Figure 1(a) shows a flips time series of a very low drive case for L = 200 and $P_0L^2 = 0.2$. As seen in the inset plots, the characteristic shape of an avalanche is a trapezoid because of the rules of the sandpile. In other words, the pulse shape is due to the lowest level physics of the system. These trapezoids are the building blocks of the sandpile time series. An avalanche grows in size with time; this corresponds to the left sloping edge of the trapezoid. Once it reaches its maximum size the avalanche either immediately shrinks or stays the same size for a number of time steps; this latter case corresponds to the flat part of the trapezoid. In either case, the avalanche shrinks in size with time until it ends; this process corresponds to the right sloping edge of the trapezoid. Now the flips are zero again, indicating no unstable cells in the sandpile. Notice that no spatial information is conveyed by a flips time series. An avalanche in the sandpile can move up the pile, down the pile or stay in the same location as it grows and then shrinks in size. Also, multiple avalanches can occur simultaneously in distant regions of the system (though not typically in the low drive case). But each of these examples can appear identical in the flips time series (Figure 1(b)).

The power spectrum and R/S analysis for flips time series of different sizes of sandpile are shown in Figure 2. Five distinct regions are seen in the power spectrum and six in the R/S. We label the different regions and breakpoints as in the sketches in Figure 3 and analyze them below. The cartoons are drawn in the spirit of Figure 6 of Reference [19]. Short annotations indicating the cause of each region are printed on each cartoon. The most interesting and significant region is the SOC region D: it is the only region that is due simply to long time correlations in the system. Though SOC implies more than just long time correlations, that specific characteristic is at the root of region D so our naming convention in this paper is to refer to this region as the SOC region. To fully understand its causes, we first explain regions A, B and C.

A. Regions A and B: pulse shapes

In the spectrum, regions A and B scale as $\sim f^{-\beta}$ with $\beta \approx 3.4$ and $\beta \approx 2$. These regions are due to the single trapezoidal pulses that represent avalanches in the time series. This was noted for the high drive case in [19] for a single region A but here we add to that an analysis of the slopes and breakpoints of both regions. To isolate the effect of the pulses from the dynamics, we randomly shuffle the time series, keeping the trapezoids intact but placing them randomly in time. The spectrum and R/S analysis are both shown in Figure 4, along with the spectrum of the original unshuffled time series. The spectra and R/S plots of the shuffled and SOC data are identical at short time scales because they share identical shapes. That the values of $T_{\rm B}^{-1}$ from the two series—SOC and shuffled—are identical says that the reason is not due to dynamics but instead to the shapes of the pulses.

The R/S analysis shows a strongly correlated Hurst exponent, $H \approx 0.9$, up to $T_{\rm B}$ because a defined shape, such as a trapezoid, is correlated with itself up to its width. There is no breakpoint between regions A and B

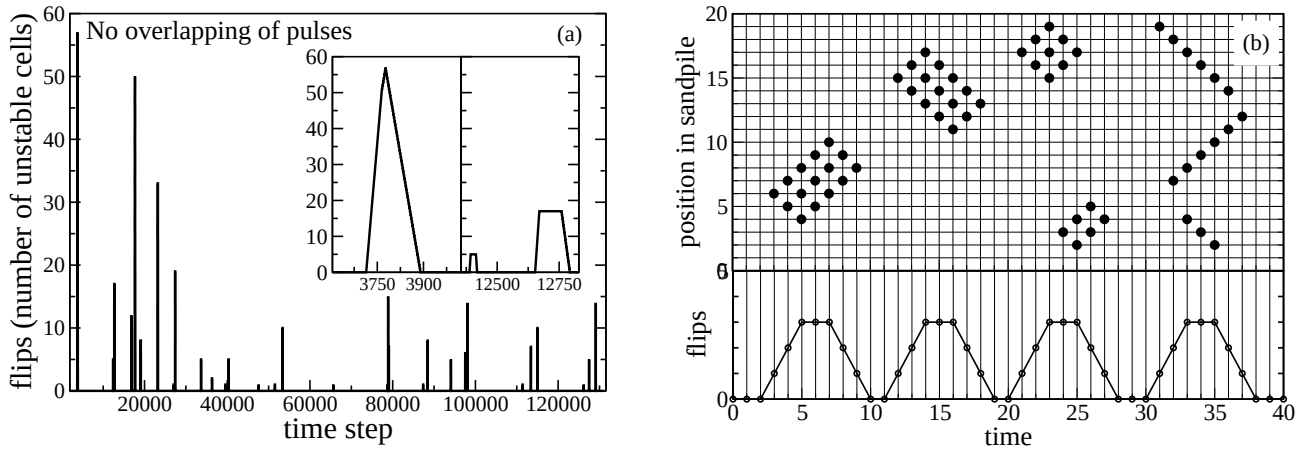

FIG. 1: Partial flips time series from running sandpile model for low drive and space-time diagram and flips time series of separate avalanches. There are approximately 30 distinct and separated events in $\sim 10^6$ time steps. In space-time diagram, solid circles in upper figure represent unstable (avalanching) cells. Flips time series, lower figure, is a record of total number of unstable cells at each time step. Structures in flips time series do not give information of location, size, number or direction of avalanches, since the same structure can be produced in multiple ways.

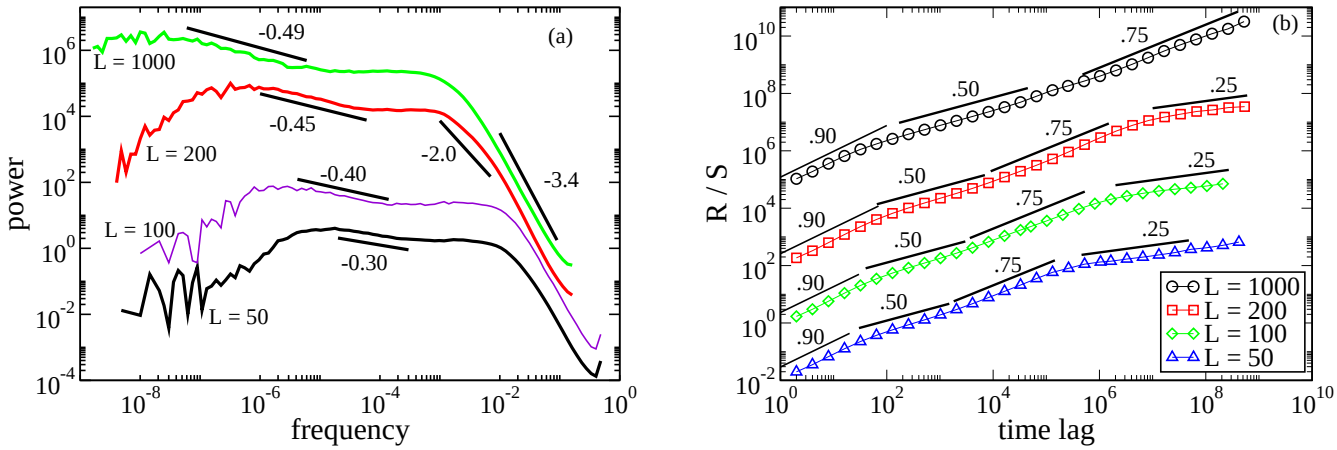

FIG. 2: Power spectra and R/S analysis of flips for low drive sandpile for $P_0L^2 = 0.2$ and L $= 50, 100, 200, 1000$. Plots have been shifted along the y axes for better viewing. The solid lines are power laws plotted with the labeled exponent; they are not fits to the data.

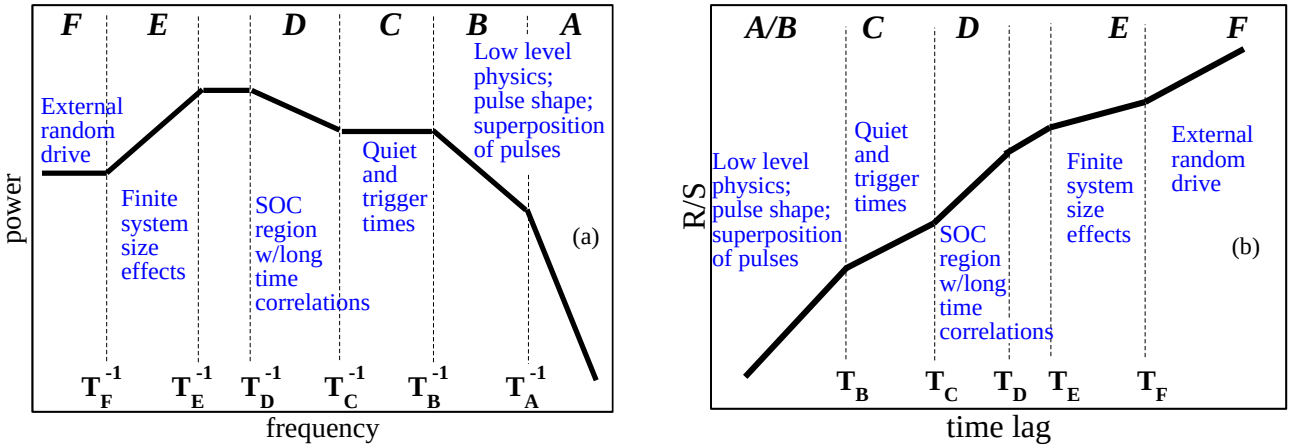

FIG. 3: Cartoons of distinct regions and their breakpoints and causes of power spectra and R/S analysis of sandpile flips.

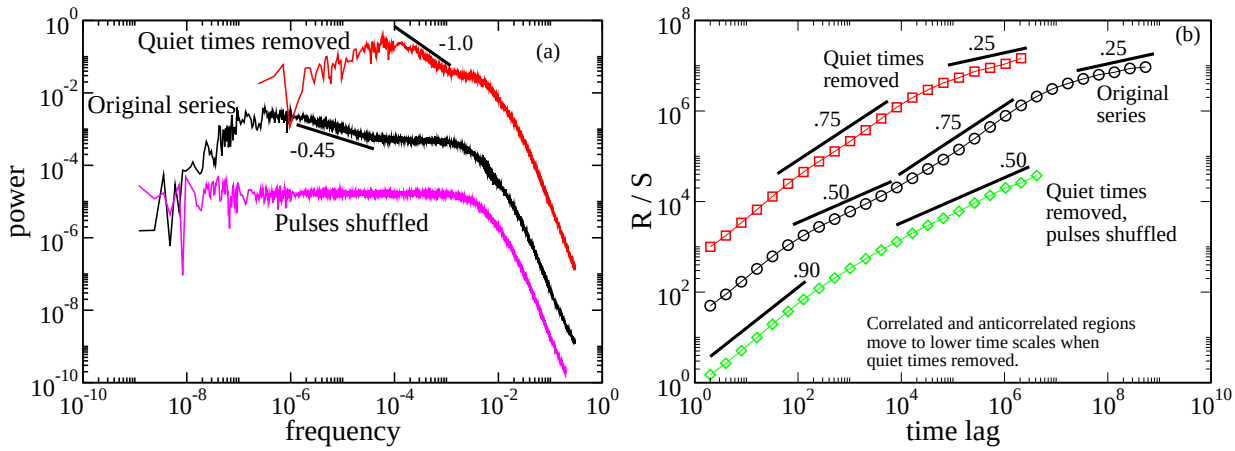

FIG. 4: Power spectra and R/S analysis of low drive sandpile: original series, with quiet times removed and with pulses shuffled. Plots have been shifted along the y axes for better viewing. The solid lines are power laws plotted with the labeled exponent; they are not fits to the data.

in the R/S analysis because this only measures correlations not shape. We test this by replacing all trapezoids in both time series with rectangles of the same width and height as the corresponding trapezoid. The resulting R/S analysis is unchanged, since it still simply measures the correlations of the pulses with themselves. The cutoff $T_{\rm B}$ (and $T_{\rm B}^{-1}$) remains the same as before since the widest pulse has not changed. The only difference is in the power spectrum, where regions A and B are replaced by a single region that scales as f^{-2}. This is a demonstration of the results of [21] and [22].

Three features must be discussed to fully explain the high frequency regions of the spectrum: 1) the breakpoint $T_{\rm B}^{-1}$ between regions C and B; 2) the presence of two power law scaling regions above $T_{\rm B}^{-1}$ and the breakpoint between them; and 3) the slopes of regions A and B. Breakpoint $T_{\rm B}^{-1}$ is due to the average duration of an avalanche, the two power law regions A and B are due to the trapezoidal pulse shape of an individual avalanche and the slopes of these two regions are due to the superposition of many nonoverlapping individual avalanches (trapezoids).

To explain these high frequency regions, we note that the power spectrum of a single trapezoid of width $W = 2(a+b)$ and height A, as defined in Figure 5, is

$$P_{\rm trap}(\omega) = |F_{\rm trap}(\omega)|^2 = \left\{ \frac{2A}{b\omega^2} \left[\cos(\omega a) - \cos\left(\omega(b+a)\right) + b\omega \sin(\omega a)\right] \right\}^2 .$$

For convenience, we have used $\omega = 2\pi f$. The scaling behaviour of this function depends upon the ratio a/b. When $a/b \lessapprox 1$ the trapezoid is more triangular and two scaling regions of ω^0 and ω^{-4} appear with a breakpoint between them at $\omega \approx W^{-1} \approx b^{-1}$. (Figure 5). When $a/b \gg 1$ the trapezoid is more rectangular and three scaling regions appear with two breakpoints, $\omega_1 \approx W^{-1} \approx a^{-1}$ and $\omega_2 \approx b^{-1} > a^{-1}$. As in the more triangular case, the lowest and highest regions scale as ω^0 and ω^{-4}, respectively but in the new middle region the spectrum scales as ω^{-2}.

Since there are three scaling regions in the sandpile spectra that scale similarly to those of a single trapezoid, we conclude that most of the avalanches have durations much longer than the sum of their growth and decay times, as this is the $a/b \gg 1$ condition for a trapezoid. Therefore the first breakpoint $T_{\rm B}^{-1}$ must be a measure of the average duration. $T_{\rm B}$ is on the same order as but less than L, since the majority of avalanche durations will be less than the system size. (Some can be larger because occasional large continuous events propagate up and down the sandpile, like waves sloshing back and forth in a tank.)

The slope of the spectrum in region A (≈ 3.4) is flatter than that found for a single trapezoid ($= 4$) because of a process that 'contaminates' the f^{-4} spectrum with f^{-2}

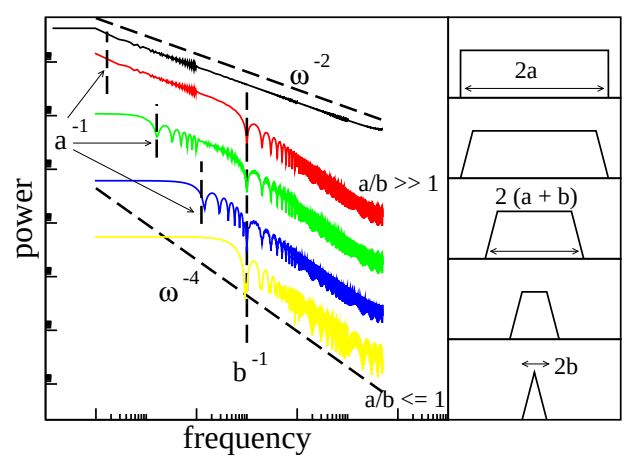

FIG. 5: Cartoon definitions of trapezoidal, rectangular and triangular pulses and power spectra of 5 trapezoids with changing a and b.

and f^0 contributions. Not all of the trapezoids in the time series are of width $T_{\rm B} \approx$ L. Most are smaller so that the cutoff in frequency space for their spectra will be at higher frequencies. That is, the cutoff due to, say, a trapezoid of width L/n occurs at n times the frequency of that due to a large trapezoid of width L. This means that the f^{-2} and f^0 regions of the smaller pulses occur at higher frequencies and tend to reduce $\beta = 4$ of the larger pulses. While this flattens the slope in region A it does not do the same in region B.

Before leaving regions A and B we address two of the assumptions of [21] and [22]: 1) events are well-approximated as rectangular pulses and 2) events in a superposition are *random* and independent. These assumptions are not appropriate for the flips time series of a SOC sandpile model. The first of these is contradicted by the high frequency $\beta \approx 3.4$ region of the sandpile spectrum. If the fundamental pulse shape were rectangular, then this region would be a continuation of the middle $\beta \approx 2$ region; there would be only two regions (counting the flat one for $\omega \ll \omega_0$). This is not just trivia or a pedantic argument to stake a claim for the 'proper' pulse shape for the sandpile. Instead, it is a statement of the lowest level physics of the system. The high frequency regions of the sandpile spectrum scale as they do because of the trapezoidal pulse shapes. Similarly, the spectra of systems (SOC or otherwise) with different low level physics and different fundamental pulse shapes may scale differently.

We have already touched on the other assumption, that events in a superposition are random and independent. This is not the case in the SOC sandpile, as shown by the comparison of the spectra of shuffled and unshuffled pulses in Figure 4. Memory stored in the sandpile gradients create correlations among avalanches. For this very low drive case, the difference in spectra due to this memory appears at very low frequencies; we will discuss this further in Section IV C. But since at high frequencies (short time scales) the spectra of correlated pulses are identical to the spectra of random pulses and since before this study the necessary long, low-drive time series had not been seen, this assumption of randomness had made sense.

B. Region C: quiet times

This is a region not previously described; it is due to quiet times, which are periods with no avalanches [25, 26]. Region C scales as f^0 in the power spectrum and as $H \approx 0.5$ in the R/S analysis, both signatures of an uncorrelated process. This region reflects the random external addition of sand to the system, where avalanches are randomly triggered. Beyond the time scale of the largest single avalanche, $T_{\rm B}$, there can be a period where the correlations are dominated by the random triggering. The width of region C is inversely related to the driving rate. Thus, the lower the driving rate, the fewer avalanches occur in a given time period and the longer the system must wait for enough avalanches to occur to correlate with each other. The cutoff, $T_{\rm C}$, is a measure of a minimum time needed for enough avalanches to occur that are correlated with each other.

Since the power spectrum is also the Fourier transform of the autocorrelation function, visualizing the autocorrelation process can help in understanding why the spectrum is flat and $H \approx 0.5$ on these time scales. Consider a time series of length $T_0 \approx T_{\rm C}$ from the low drive sandpile. This series consists of trapezoidal pulses, representing avalanches, alternating with flat quiet time regions, representing inactivity in the sandpile. Now picture the autocorrelation process, where a copy of the series is shifted by a time lag τ and multiplied by the original series; the resulting product is then summed. Up to a time lag $\tau \approx T_{\rm B}$, pulses overlap with themselves, producing the correlations of regions A and B described in Section IV A. But since average quiet times $T_{\rm C}$ are longer than average avalanche durations $T_{\rm B}$, for time lags $T_{\rm C} \gtrapprox \tau \gtrapprox T_{\rm B}$ pulses in the shifted copy of the series now overlap quiet times in the unshifted series. When these two series are multiplied, the pulses are cancelled by the quiet times. This is, of course, an average behaviour in the same way that in a truly random time series, troughs and peaks cancel each other out on average in the autocorrelation. The difference now is that for time lags $\tau > T_{\rm C}$ (and for a longer time series), the pulses begin to correlate with other pulses that occur, on average, more than $T_{\rm C}$ time steps later. This correlation is due to the memory stored in the local sandpile gradients, discussed below.

Even if the quiet times were greatly reduced or completely removed, correlations would not immediately begin at $T_{\rm B}$ because successive avalanches in time usually take place in different spatial regions of the sandpile. These spatially separated but temporally close events do not affect each other on short time scales. But an avalanche does affect the next event that occurs in the same spatial neighborhood. Analogously (and simplistically), one might assume that a small earthquake located at one end of a 1,000 kilometer fault is not related to one that occurs one hour later at the other end of the same fault. However, through a local shift in stress/strain the first temblor is almost surely connected to another earthquake only 10 kilometers away that also occurs one hour later.

We test this by removing all of the quiet times from the flips time series and comparing the spectra of the two series (Figure 4). Regions A and B are unchanged since the same shapes are still in both series. Region C has been essentially eliminated, though a vestige of its former self remains because correlations among successive events do not usually occur. In the R/S analysis, this region is too small to be identified when the quiet times are removed. The region's disappearance in R/S is consistent with its shrinkage in the spectrum.

This test also reveals the link between the running

sandpile and the zero drive sandpile of [35], where the addition of sand is suspended during an active avalanche. The spectrum and R/S analysis of the zero drive case are identical with those of the low drive case with quiet times removed. This makes sense, since the zero drive sandpile has very few quiet times by construction, as sand is always added during a time step when there is no avalanche. This prevents long periods of inactivity. In contrast, in the running sandpile there is always a finite probability of a grain of sand *not* falling during a time step. Since at low drive this probability increases, quiet times can become quite large. The important similarity between the two cases, though, is that there are few or no overlapping avalanches. When an avalanche is initiated the probability is low (nonexistent in the zero drive case) that another avalanche will initiate before the first one ends. We emphasize this to introduce the next section, which shows that overlapping of events is not necessary to produce correlated dynamics.

C. Region D: SOC and correlated events

The physics of this region is the main point of this paper. Region D is the only true dynamical SOC region in the sense that its signatures arise solely from interactions and correlations among separate events in the system. *On the time scales in this region, the signatures reflect only long time correlations and nothing about pulse shape, quiet times, random superpositions, overlapping of pulses or system size.* Because the high frequency end of this region is due to driving rate and the low frequency end is due to the finite capacity of the sandpile, larger systems have larger regions D. The limiting extension is that a system of infinite size would have a region D that extends to infinitely low frequencies and there would be no regions E or F.

For all cases in the low drive regime, regardless of system size, we find $H \approx 0.75$ in region D, indicating long time correlations among distinct and separate events. This region exists on time scales far greater than the maximum duration of an individual avalanche (T_{B}) so the correlations must arise from the interactions among those distinct events. But since there is no (or very little) overlapping in the low drive regime the correlations must be due to the specific order of events that occur in the sandpile. This order is due to memory in the system.

Memory in the sandpile is retained in the heights (and, therefore, the local gradients) of each cell. Since quiet times are the lack of any activity, they play no role in the memory. That is, whether quiet times are left to evolve naturally or are completely removed or are even imposed artificially and randomly (with a Poisson distribution) between events, the same sequence of avalanches (statistically) will occur based on the dynamical rules of the sandpile. If quiet times grow extremely long because the drive is so low then this simply means that region C will extend to lower frequencies before the inevitable region D begins. On the other hand, if quiet times grow either very short or nonexistent, because of high drive, then the simple pulses discussed here will overlap, leading to a regime with different characteristics (see [34]).

Still, though, how does this memory lead to positive correlations? This question is equivalent to: why does an avalanche now increase the probability of an avalanche later even though the random drive is unchanged? Consider the initiation of an avalanche, which, by definition, occurs after a quiet time when a grain of sand from the random external drive is added to a cell n that has slope $Z_{\mathrm{n}} = Z_{\mathrm{crit}} - 1$. After the addition of sand, that cell is critical and it then relaxes to $Z_{\mathrm{n}} = Z_{\mathrm{crit}} - N_{\mathrm{f}}$ by dumping N_{f} grains to the cell below. The slope in cells $n-1$ and $n+1$ have increased by N_{f} as flux is transported down the gradient. If either of their slopes were greater than $Z_{\mathrm{crit}} - N_{\mathrm{f}}$ before this toppling, then one or both of them are now critical and the avalanche continues to propagate up and/or down the sandpile. If, however, their slopes were less than $Z_{\mathrm{crit}} - N_{\mathrm{f}}$, then the avalanche would stop but their slopes would be closer to critical by an amount N_{f}, making an avalanche more likely to occur there the next time sand is added (Figure 6).

This is the root of the positive correlation: when an avalanche ends, the cells at the endpoints of its active zone are closer to critical and are more likely to be the initiation point of another avalanche. This, also, is the basis for memory in the system: a cell "remembers" that an avalanche just stopped there and "knows" that it will initiate an avalanche with the next slope increase from either random drive or from another neighboring avalanche. *Regardless of how long the intervening quiet time is between two events, they are correlated in the same way.* Such a process can easily be pictured for a natural system, where disturbances propagate to some finite extent and leave the gradients at their endpoints greater than before the event.

Though events are triggered at random intervals, *the event time series is not random.* That is, correlations exist among separate events. We show this by using the time series of shuffled pulses as before, Figure 4. Regions C, D, E and F collapse into a single uncorrelated region for all time scales beyond T_{B}, where the shuffled series is seen to have a f^0 spectrum down to the lowest frequencies and a Hurst exponent $H \approx 0.5$ to the longest time scales. This is in contrast to the spectrum of the sandpile series, which shows structure in the spectrum at low frequencies and $H \neq 0.5$ at long time scales. A random time series is known to have a spectrum that scales as f^0 and $H = 0.5$ so this shows that the SOC series is not simply a random superposition of pulses.

This is remarkable. Given N pulses from a power law pdf in a time series there are $N!$ possible ways in which they can be ordered. The sandpile dynamically selects one of just a relatively few such orderings that give correlations and structure in the R/S analysis and spectrum.

To show that the correlations are among the separate events and that quiet times have no role in these corre-

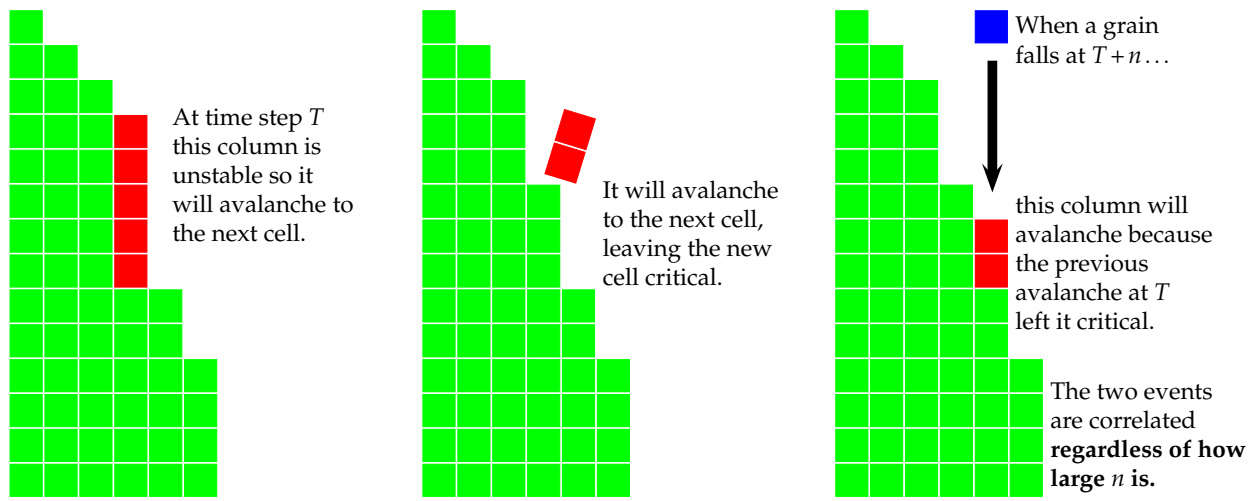

FIG. 6: Correlations between avalanches because of memory in local gradients.

lations, we return to the time series with all quiet times removed. As seen in Figure 4, region C disappears. That is, the $H \approx 0.5$ region is replaced by a $H \approx 0.75$ region. We take this to mean that the $H \approx 0.75$ region D of the original data (with quiet times) has moved to shorter time scales due to the removal of quiet times and the concomitant shortening of the series. But the correlations among events must remain the same since neither their order nor their sizes have changed. Only their frequency is different and this is reflected in the same $H \approx 0.75$ region at shorter time scales. This value of H holds for this region regardless of system size or driving rate, indicating that $H \approx 0.75$ is a robust signature of SOC dynamics.

Understanding the power spectrum for this region is not as simple as for the R/S analysis. The slope of this region, β, changes with driving rate and with system size, as well as with the removal of quiet times. As an example case, we examine a sandpile of L = 200 and $\overline{J_{\rm IN}} = 10^{-3}$ and see that $\beta \approx 0.45$. For the first of the two tests above, shuffling the pulses, we see similar behaviour to that in the R/S analysis. Namely, region D disappears or merges with regions C, E and F, leaving one large region of spectrum that scales as f^0, the signature of uncorrelated random noise. Again, shuffling the individual avalanches destroys the sandpile-selected order and eliminates all long time correlations.

The results of the second test are more interesting: removing the quiet times produces a $1/f$ region. That is, when quiet times are eliminated, the correlations among the events go to shorter time scales (higher frequencies), as described above. But the slope of region D changes from $\beta \approx 0.45$ to $\beta \approx 1$.

This implies that a $1/f$ region is not a necessary signature of SOC dynamics. But the SOC dynamics and events that produce a $1/f$ signature are present at low drive when the $f^{-\beta}$ region appears with $\beta < 1$. Even as β changes, though, the Hurst exponent remains constant.

Recall that the low drive case with quiet times removed was shown to be dynamically equivalent to the zero drive case. Now we see that this zero drive case, which is the original 1D model of [1, 2], modified by [35] to restrict $N_{\rm f} > 1$, does contain a $1/f$ region. The search for an explanation of such a region was one of the original motivations behind SOC.

Since the same correlations among the same events still hold, we interpret this behaviour of β and H to indicate that R/S analysis is a more robust measure of correlations among events than the power spectrum. The spectrum, though, may be a good measure of amount of overlap and/or effective drive.

The question of why the slope of region D in the spectrum changes to $1/f$ when the quiet times are removed is puzzling. It is not due to the conservation of the integrated power of the shorter time series; this can be calculated using the Parseval-Rayleigh Theorem [36]. Though not yet completely understood, we feel that this change lies at the root of the $1/f$ question. We discuss the issue of changing β and constant H further in [34].

D. Region E: anticorrelated events

This is the discharge event region well-studied by [19] for high drive. The same process drives both the low and high drive cases, namely the finite capacity sandpile eventually fills up and empties out in great system-wide discharges. (Again, a sandpile of infinite size would not have this region.) The finite sandpile is always being driven towards a globally critical slope. Once all or almost all cells have slope $Z_{\rm crit} - 1$, a keystone toppling, usually near the bottom, will produce a system-size avalanche or a rapid succession of smaller avalanches that removes enough sand so that the slopes at all sites are reduced to much less than critical ($\approx Z_{\rm crit} - N_{\rm f}$). Once such a large event occurs, it is unlikely that one will happen again for a long time. Hence, large events are anticorrelated;

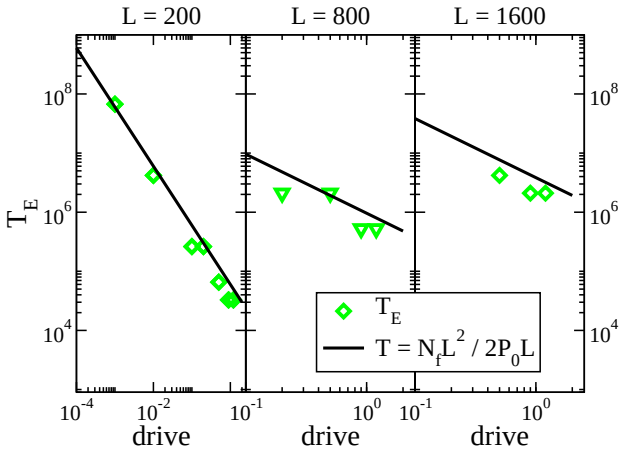

FIG. 7: Breakpoint of beginning of anticorrelated region versus driving rate for three different system sizes. Solid lines are $T = \frac{N_f L^2}{2P_0 L}$

the signature of anticorrelated dynamics is $\beta < 0$ in the spectrum and $H < 0.5$ in R/S analysis. Both signatures are seen in the sandpile.

Note that these large discharge events are not necessarily a single avalanche. While such an event is possible, a discharge event can comprise many smaller avalanches that occur over a short time span. The key point is that both types of discharge events effectively reset the system by relaxing the near-critical local gradient to much less than critical at all or most locations.

After a discharge event, the sandpile fills up, on average, in at least $T_{\rm E}$ and at most $T_{\rm F}$ time steps, so the breakpoints defining this region can be calculated. The maximum sandpile capacity is $C_{max} = \frac{Z_{\rm crit} L^2}{2}$. After a systemwide event, the total mass is reduced to approximately $C_{min} = \frac{(Z_{\rm crit} - N_{\rm f}) L^2}{2}$. The minimum time needed to refill to maximum is then $T_{\rm re,min} = \frac{N_{\rm f} L^2}{2P_0 L}$. This expression is plotted in Figure 7 and is seen to agree with the breakpoint data of $T_{\rm E}$ versus $P_0 L$.

The above $T_{\rm re,min}$ is a minimum time and, hence, is related to a maximum frequency, $T_{\rm E}^{-1}$. To calculate the minimum frequency, $T_{\rm F}^{-1}$, we notice that since sand continues to leave the sandpile at the bottom during the refilling process, $T_{\rm refill}$ is usually greater than $T_{\rm re,min}$. Though the sandpile is in steady state in the longest time scales, at some smaller ones flux into the system exceeds flux out. The reason for this is that sand falls into all cells with equal probability from the random drive but sand can only leave the system through the bottom cell. In the SOC region D, there is a finite time and a convoluted path for sand to travel from where it initially lands to where it exits at the bottom. This time is much slower when the system as a whole is farther from critical (region D). But once all cells are critical, this time is much shorter and one large avalanche (or rapid succession of many) is the very efficient mechanism that quickly removes much mass and keeps the sandpile in a steady state over the longest time scales. At this point, though, we have not derived breakpoint $T_{\rm F}$.

Beyond breakpoint $T_{\rm F}^{-1}$, at the lowest frequencies, the spectrum is flat; the following is conjecture about its cause and limits. The flat spectrum is a reflection of the random drive of the system on the longest time scales since all dynamics is on time scales much smaller than those in this region. This is the extent of the memory process discussed in regards to region D. That memory is eventually erased by the system-wide events which tend to destroy the record of events stored in the heights of each cell. The memory is shuffled by the random drive at time scales longer than $T_{\rm F}$. Region F extends to infinitely low frequencies; there are no further dynamical regions below it.

V. CONCLUSIONS

We have studied the one dimensional directed running sandpile at very low drive and have shown that correlations from a memory mechanism in SOC dynamics produce nontrivial signatures in the power spectra and R/S analysis of flips time series. The memory is stored in the local gradient of each cell, regardless of driving rate. The signatures of the correlations appear at longer time scales for lower external forcing. A consequence of this is that a time series for any system, be it a defined SOC model or a real physical system suspected of being SOC, can be too short to see the correlation signatures and thus could be mistaken for a simple random time series. Given long enough time series, a very distinct difference can be seen between the signatures of random data and the sandpile data. The sandpile chooses the particular size, order and separation of events in a way that is very different from any random combination of size, order and separation.

Multiple distinct power law regions are found in spectral and rescaled range analysis of the SOC avalanche time series but only one of these (region D) is due solely to correlations among events. Its signature is a power law region in the spectrum that scales as $f^{-\beta}$ with $0 < \beta \leq 1$ and a Hurst exponent $H \approx 0.75$. An infinite sandpile would have infinite capacity and, thus, have no discharge events. Therefore the SOC region D would extend to infinitely long time scales.

Part of the allure of SOC has been the lack of tuning required for the system to be critical. By probing the low drive system at very long times we have shown that overlapping of events and, therefore, tuning of the external forcing is not necessary in order to have SOC dynamics. Regions of nontrivial $f^{-\beta}$ are seen at very low frequencies. This indicates that in a SOC system *avalanches always correlate over very long times even when they do not overlap in time.* It also shows that tuning of the drive is not necessary for a SOC system to be in its self-organized critical state, as the memory mechanism is always present in the gradients regardless of how slowly or quickly sand is added.

Signatures of these long time correlations in the form of power laws in the spectra and R/S analysis are present at all drives. In a sense, the signatures at low drive are more fundamental than those at high drive because the actual time series are composed of the basic non-overlapping events of the SOC system. These events contain all of the relevant dynamics and are the building blocks to which the title refers.

Acknowledgments

Many thanks to N. W. Watkins, B. T. Werner and H. J. Fletcher for support and suggestions.

[1] P. Bak, C. Tang, and K. Wiesenfeld, Phys. Rev. Let. **59**, 381 (1987).
[2] P. Bak, C. Tang, and K. Wiesenfeld, Phys. Rev. A **38**, 364 (1988).
[3] P. Bak, *How Nature Works* (Springer-Verlag, New York, 1996).
[4] H. J. Jensen, *Self-organized criticality: emergent complex behaviour in physical and biological systems* (Cambridge University Press, Cambridge, 1998).
[5] J. Davidsen and M. Paczuski, Phys. Rev. E **66**, 050101(R) (2002).
[6] A. Vespignanni and S. Zapperi, Phys. Rev. E **57**, 6345 (1998).
[7] D. E. Newman, B. A. Carreras, P. H. Diamond, and T. S. Hahm, Phys. Plasmas **3**, 1858 (1996).
[8] B. A. Carreras, D. Newman, and V. E. L. et al., Phys. Plasmas **3**, 2903 (1996).
[9] B. A. Carreras, B. P. van Milligen, and M. A. P. et al., Phys. Rev. Let. **80**, 4438 (1998).
[10] L. Garcia, B. A. Carreras, and D. E. Newman, Phys. Plasmas **9**, 841 (2002).
[11] T. S. Chang, Phys. Plasmas **6**, 4137 (1999).
[12] S. C. Chapman and N. W. Watkins, Space Sci. Rev. **95** (2001).
[13] R. Woodard, D. E. Newman, R. Sánchez, and B. A. Carreras (2004), accepted for publication in Proceedings of Conference on Sun-Earth Connection: Multiscale Coupling in Sun-Earth Processes, Kona, Hawaii.
[14] D. L. Turcotte, *Fractals and Chaos in Geology and Geophysics* (Cambridge University Press, 1997), 2nd ed.
[15] B. Carreras, V. E. Lynch, I. Dobson, and D. E. Newman, Chaos **12**, 985 (2002).
[16] B. Carreras, D. Newman, I. Dobson, and A. Poole, IEEE Trans. on Circuits and Systems, Part 1 (2004), accepted March 200.
[17] B. Carreras, V. E. Lynch, I. Dobson, and D. E. Newman, Chaos (2004), accepted June 2004.
[18] D. E. Newman, B. A. Carreras, N. D. Sizemore, and V. E. Lynch, in *35th Hawaii International Conference on System Sciences* (Hawaii, 2002).
[19] T. Hwa and M. Kardar, Phys. Rev. A **45**, 7002 (1992).
[20] URL `http://www.nslij-genetics.org/wli/1fnoise/`.
[21] H. J. Jensen, K. Christensen, and H. C. Fogedby, Phys. Rev. B **40**, 7425 (1989).
[22] J. Kertész and L. B. Kiss, J. Phys. A **23**, L433 (1990).
[23] S. S. Manna, J. Phys. A **24** (1991).
[24] P. H. Diamond and T. S. Hahm, Phys. Rev. Let. **2**, 3640 (1995).
[25] R. Sánchez, D. E. Newman, W. Ferenbaugh, B. A. Carreras, V. E. Lynch, and B. P. van Milligen, Phys. Rev. E **66**, 036124 (2002).
[26] R. Sánchez, D. E. Newman, and B. A. Carreras, Phys. Rev. Let. **88**, 068302 (2002).
[27] H. E. Hurst, Trans. Am. Soc. Civ. Eng. **116**, 770 (1951).
[28] B. B. Mandelbrot, *Multifractals and* $1/f$ *noise* (Springer-Verlag, 1999).
[29] B. B. Mandelbrot, *Gaussian self-affinity and fractals* (Springer-Verlag, 2002).
[30] M. J. Cannon, D. B. Percival, D. C. Caccia, G. M. Raymond, and J. B. Bassingthwaighte, Physica A (1997).
[31] C.-K. Peng, S. V. Buldyrev, S. Havlin, M. Simons, H. E. Stanley, and A. L. Goldberger, Phys. Rev. E **49**, 1685 (1994).
[32] C. X. Yu, M. Gilmore, W. Peebles, and T. Rhodes, Phys. Plasmas **10**, 2772 (2003).
[33] B. M. Gammel, Phys. Rev. E **58**, 2586 (1998).
[34] R. Woodard, D. E. Newman, R. Sánchez, and B. A. Carreras (2004), in preparation for submission to PRE.
[35] L. P. Kadanoff, S. R. Nagel, L. Wu, and S. min Zhou, Phys. Rev. A **39**, 6524 (1989).
[36] R. N. Bracewell, *The Fourier Transform and Its Applications* (McGraw-Hill, 2000), 3rd ed.